Journal of
Materials Chemistry A

Accepted Manuscript

This article can be cited before page numbers have been issued, to do this please use: J. Wang, X. Bao, D. Ding, M. Qiu, Z. Du, J. Wang, J. Liu, M. Sun and R. Yang, *J. Mater. Chem. A*, 2016, DOI: 10.1039/C6TA04059D.

ROYAL SOCIETY OF CHEMISTRY

www.rsc.org/materialsA

View Article Online
DOI: 10.1039/C6TA04059D

Journal of Materials Chemistry A

ARTICLE

Fluorine-induced high-performance narrow bandgap polymer based on thiadiazolo[3,4-*c*]pyridine for photovoltaic application†

Received 00th January 20xx,
Accepted 00th January 20xx

DOI: 10.1039/x0xx00000x

www.rsc.org/

Jiuxing Wang,[a,b] Xichang Bao,*[,a] Dakang Ding,[a,c] Meng Qiu,[a] Zurong Du,[a,b] Junyi Wang,[a,b] Jie Liu,*[,a] Mingliang Sun[c] and Renqiang Yang*[,a,d]

Thiadiazolo[3,4-*c*]pyridine (PT) has great potential in constructing high-performance narrow bandgap (NBG) photovoltaic polymers. But to date the best power conversion efficiencies (PCEs) for PT-containing polymers are only around 6%. Herein we report two PT-containing NBG polymers PDTPT-2T and PDTPT-2TF based on 2,2'-bithiophene (2T) and 3,3'-difluoro-2,2'-bithiophene (2TF), respectively. The effects of fluorine substituent on optoelectronic properties are thoroughly investigated. The film absorption onset of PDTPT-2TF is 855 nm, bathochromic-shifted by 24 nm in comparison with that (831 nm) of PDTPT-2T. The lowest unoccupied molecular orbital (LUMO) and highest occupied molecular orbital (HOMO) energy levels of PDTPT-2TF are down-shifted by 0.15 and 0.11 eV relative to those of PDTPT-2T, respectively. X-ray diffraction (XRD) patterns indicate that more ordered structure is formed in the solid film of PDTPT-2TF. Furthermore, the miscibility between polymer and [6,6]-phenyl-C_{71}-butyric acid methyl ester ($PC_{71}BM$) is significantly improved through the introduction of fluorine. Consequently, PDTPT-2TF exhibits a high PCE of 8.01% while PDTPT-2T only shows a maximum PCE of 2.65%. The efficiency of 8.01% is the highest one for PT-containing polymers, and more importantly, it is achieved without any processing additives or post-treatments. This work indicates that PT would have great potential as building block to construct high-performance photovoltaic polymers.

Introduction

Polymer solar cells (PSCs) have generated significant interest due to their potential in fabrication of large-scale flexible devices through low-cost solution processing techniques.[1-4] During the last decade, remarkable progress has been made in enhancing the power conversion efficiency (PCE) of the PSCs, such as development of high-performance polymer donors,[4-14] incorporation of efficient interfacial materials,[15-17] and advancement of device architectures.[18,19] Despite plenty of high-performance polymer donors having been reported, only a limited number of them are narrow bandgap (NBG, < 1.50 eV) polymers.[6,20-23] Compared with large and medium bandgap polymers, NBG polymers have strong and broad absorption in near-infrared region, which makes them an important component for constructing multicomponent and tandem solar cells.[21,24-26] However, most reported high-performance NBG polymers usually need complex morphology engineering and interfacial modifications during device fabrications, which may limit their further applications.[6,20-22,27] Therefore, it's necessary to develop novel high-performance NBG polymers with easy device processing methods and simple device structures.

An effective strategy to design NBG polymer is to incorporate alternating electron-rich and electron-deficient moieties along the backbone of the conjugated polymer.[1,28,29] Compared with the widely used acceptor unit benzothiadiazole (BT), thiadiazolo[3,4-*c*]pyridine (PT) has a stronger electron-withdrawing ability.[30-32] Polymers containing PT usually have broader absorption spectra extending into near-infrared region.[31,33-35] In 2010, Zhou et al. reported a series of polymers containing alkylthienyl-flanked PT (DTPT).[32] Compared with their BT counterparts, the PT-containing polymers showed smaller bandgaps and decreased lowest unoccupied molecular orbital (LUMO) and highest occupied molecular orbital (HOMO) energy levels. The best-performing PSC gave an impressive PCE of 6.32%. In 2013, Heeney and coworkers synthesized three polymers based on benzo[*d*][1,2,3]triazole (BTz), 5,6-difluorobenzo[*c*][1,2,5]thiadiazole (ffBT), and PT, respectively.[36] The PT-containing polymer exhibited the smallest bandgap and the largest short-circuit current density (J_{sc} = 19.6 mA/cm^2), in comparison with the BTz-containing polymer (J_{sc} = 6.17 mA/cm^2) and the ffBT-containing polymer (J_{sc} = 5.74 mA/cm^2). As a result, the polymer containing PT showed the highest PCE of 6.6% among the three polymers.

[a] CAS Key Laboratory of Bio-based Materials, Qingdao Institute of Bioenergy and Bioprocess Technology, Chinese Academy of Sciences, Qingdao 266101, China. E-mail: baoxc@qibebt.ac.cn; liu_jie@qibebt.ac.cn; yangrq@qibebt.ac.cn
[b] University of Chinese Academy of Sciences, Beijing 100049, China.
[c] Institute of Material Science and Engineering, Ocean University of China, Qingdao 266100, China.
[d] State Key Laboratory of Luminescent Materials and Devices, South China University of Technology, Guangzhou 510641, China.

†Electronic Supplementary Information (ESI) available: [TGA plots, temperature-dependent absorption spectra of PDTPT-2TF, HOMO and LUMO distributions, hole mobility measurements, photovoltaic performance of PDTPT-2T with additive, TEM images, ^{1}H NMR and ^{13}C NMR spectra]. See DOI: 10.1039/x0xx00000x

View Article Online
DOI: 10.1039/C6TA04059D

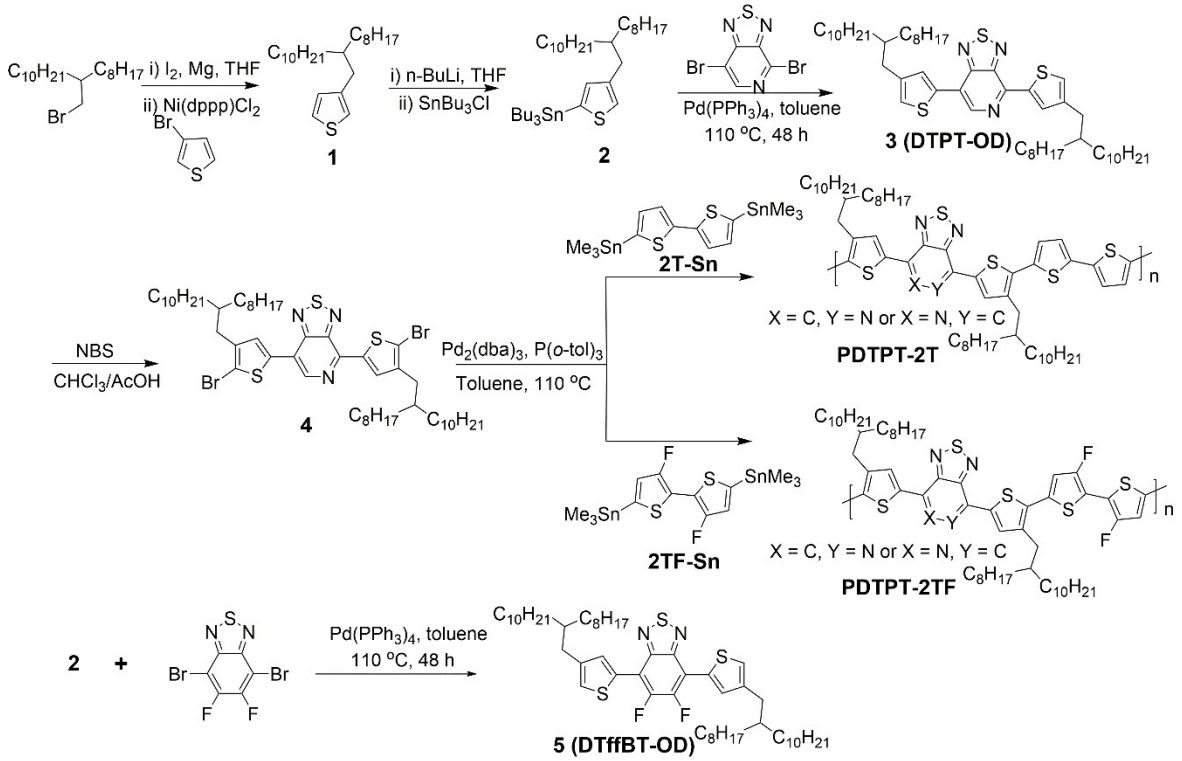

Scheme 1 Chemical structures and synthetic routes of DTffBT-OD, PDTPT-2T and PDTPT-2TF.

Previous studies indicate that PT should be a promising unit for constructing high-performance NBG polymers. However, to the best of our knowledge, none of the reported PCEs of PT-containing polymers is over 7%, implying that there is still considerable room to improve the photovoltaic performance.[32,36-43] Therefore, it is necessary and meaningful to further investigate the structure-property relationships of PT-containing polymers. Incorporating fluorine into polymer chains is usually an effective strategy to improve their photovoltaic properties. Polymers containing fluorinated units, such as ffBT,[4,5] 3-fluorothieno[3,4-*b*]thiophene (TTF),[7] and 3,3'-difluoro-2,2'-bithiophene (2TF),[5] have realized very high PCEs. But to date fluorinated polymers containing PT unit haven't been reported. In this work, we firstly applied fluorine in PT-containing polymer and thoroughly studied the effects of fluorine substituent on its optoelectronic properties. A new acceptor moiety, namely DTPT-OD (Scheme 1), was designed by introducing a long branched alkyl chain onto the 4-position of the flanking thiophene ring of DTPT to improve the solubility and molecular weight of the polymers.[32] As shown in Fig. 1, DTPT-OD exhibits obviously bathochromic-shifted and broader absorption profile in comparison with DTffBT-OD (one of the most efficient moieties for constructing photovoltaic polymers, Scheme 1), indicating a distinct advantage of DTPT-OD as building block. To make a comparative study, 2TF and 2,2'-bithiophene (2T) were chosen as the electron-rich units, respectively. Thus, two new polymers comprising DTPT-OD and 2T (named PDTPT-2T) or 2TF (named PDTPT-2TF) were synthesized. The two polymers showed noticeably different

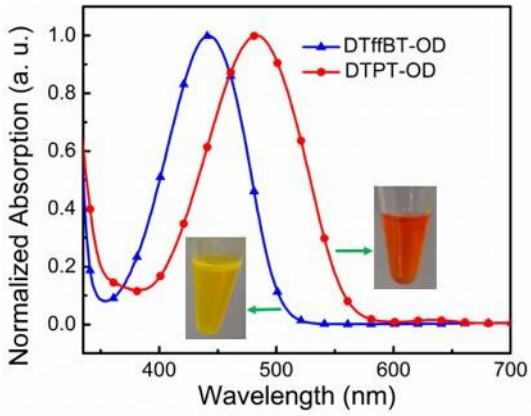

Fig. 1 Normalized absorption spectra of DTPT-OD and DTffBT-OD in $CHCl_3$ solution.

optoelectronic properties. The incorporation of fluorine significantly improved the photovoltaic performance. PDTPT-2TF exhibited a high PCE of 8.01% while PDTPT-2T only showed a maximum PCE of 2.65%.

Results and discussion

Synthesis and characterization

Scheme 1 describes the synthetic routes of PDTPT-2T and PDTPT-2TF. Detailed synthetic procedures can be found in the Experimental section. The polymers were synthesized through Stille coupling reaction. In both cases, polymerization was

View Article Online
DOI: 10.1039/C6TA04059D

rapid and the reacting solution became gel within two hours. Both polymers had a good solubility in *o*-dichlorobenzene (DCB) at heated temperature. The molecular weights of PDTPT-2T and PDTPT-2TF were measured by gel permeation chromatography (GPC). The number-average molecular weight (M_n) of PDTPT-2T is 47 kDa with a polydispersity index (PDI) of 1.67, and the M_n of PDTPT-2TF is 77 kDa with a PDI of 2.01. Thermogravimetric analysis (TGA) was performed to analyze the thermal stability of PDTPT-2T and PDTPT-2TF. As shown in Fig. S1 (Supplementary Information), PDTPT-2T and PDTPT-2TF exhibited similar thermal decomposition temperatures (T_d, 5% weight loss) of 425 °C and 427 °C, respectively. Both polymers can meet the requirements of thermal stability for photovoltaic application.

Optical properties

Normalized UV-vis absorption spectra of PDTPT-2T and PDTPT-2TF in dilute DCB solution and as solid films are depicted in Fig. 2a. Detailed optical parameters are summarized in Table 1. Both polymers showed very broad absorption extending into near-infrared region. The optical properties of the two polymers differ greatly. PDTPT-2T exhibited two absorption peaks both in solution and as solid film. From solution to film, the main peak in long-wavelength had a noticeable bathochromic-shift of 48 nm. PDTPT-2T showed no shoulder peak indicating no intense aggregations formed in solution or film. Compared with PDTPT-2T, PDTPT-2TF exhibited obviously bathochromic-shifted and broader absorption with a strong shoulder peak both in dilute solution and as solid film. The emergence of a strong shoulder peak suggests the existing of intense aggregations in PDTPT-2TF. With the increase of the temperature, the shoulder peak was gradually weakened and finally disappeared due to the disaggregation of the aggregates (Fig. S2).[9,44] The absorption spectrum of PDTPT-2TF showed no obvious bathochromic-shift from solution to film state at room temperature, which was quite different from that of PDTPT-2T. One possible explanation might be that PDTPT-2TF has already formed intense aggregations in dilute solution, which is verified in Fig. S2. The onset wavelength (λ_{onset}) of film spectrum was 831 nm for PDTPT-2T and 855 nm for PDTPT-2TF. According to the equation $E_g^{opt} = 1240/\lambda_{onset}$, the optical bandgap ($E_g^{opt}$) values were calculated to be 1.49 and 1.45 eV for PDTPT-2T and PDTPT-2TF, respectively. Incorporating fluorine onto 2T reduces the E_g^{opt} of the resulting polymer. The maximum film absorption coefficients were 5.47×10^4 and 8.50×10^4 cm^{-1} for PDTPT-2T and PDTPT-2TF, respectively, indicating that PDTPT-2TF has a stronger ability of harvesting light (Fig. 2b). From the optical features of the two polymers, it can be concluded that the incorporation of fluorine into the polymer induced to obviously enhanced intermolecular interactions, bathochromic-shifted and broader absorption, and noticeably increased absorption coefficient, which are conducive to harvesting more light.[1,8,45]

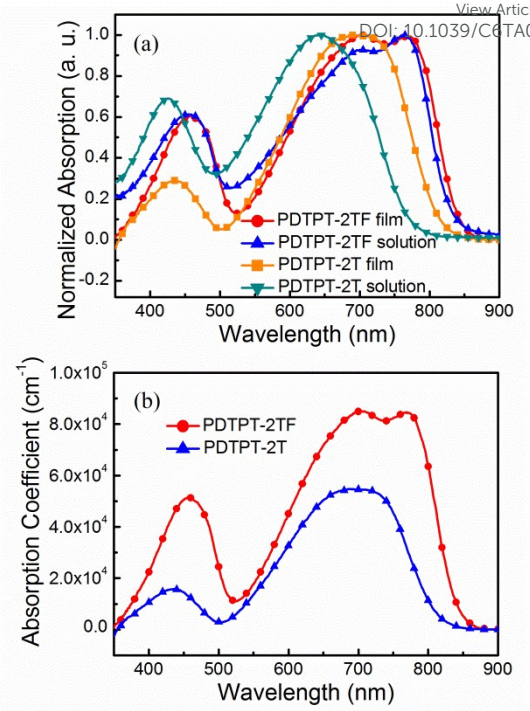

Fig. 2 (a) Normalized absorption spectra of PDTPT-2T and PDTPT-2TF in DCB solution and as solid films at room temperature. (b) Absorption coefficients of PDTPT-2T and PDTPT-2TF films.

Molecular energy levels

The HOMO energy levels of PDTPT-2T and PDTPT-2TF were estimated by cyclic volt ammetry (CV). Fig. 3 shows the cyclic voltammograms and energy level diagram of the two polymers. HOMO energy level was calculated from the equation $E_{HOMO} = -e(4.8 + E_{ox} - E_{1/2,(Fc/Fc+)})$, where E_{ox} is the onset oxidation potential of the polymer and $E_{1/2,(Fc/Fc+)}$ is the half-wave potential of the ferrocene/ferrocenium (Fc/Fc+) redox couple.[7] The value of $E_{1/2,(Fc/Fc+)}$ was calibrated to be 0.40 V vs saturated calomel electrode (SCE). The E_{ox} values obtained from the cyclic voltammograms were 0.83 and 0.94 V for PDTPT-2T and PDTPT-2TF, respectively. Thus the corresponding HOMO energy levels were -5.23 and -5.34 eV for PDTPT-2T and PDTPT-2TF, respectively. As it was difficult to record the accurate reduction potentials of the polymers, their LUMO energy levels were determined by HOMO and E_g^{opt}, using the equation $E_{LUMO} = E_{HOMO} + E_g^{opt}$. The LUMO energy levels were -3.74 and -3.89 eV for PDTPT-2T and PDTPT-2TF,

Table 1 Optical and energy level parameters of PDTPT-2T and PDTPT-2TF

Polymer	λ_{max} (nm) Solution	λ_{max} (nm) Film	λ_{onset} (nm) Film	E_g^{opt} (eV)[a]	Absorption coefficient (cm^{-1})	HOMO (eV)[b]	LUMO (eV)[c]
PDTPT-2T	425, 642	435, 690	831	1.49	5.47×10^4	-5.23	-3.74
PDTPT-2TF	455, 700, 765	457, 705, 770	855	1.45	8.50×10^4	-5.34	-3.89

[a]Calculated from the absorption onset of the polymer film. [b]Measured by cyclic voltammetry. [c]Calculated from the equation $E_{LUMO} = E_{HOMO} + E_g^{opt}$.

View Article Online
DOI: 10.1039/C6TA04059D

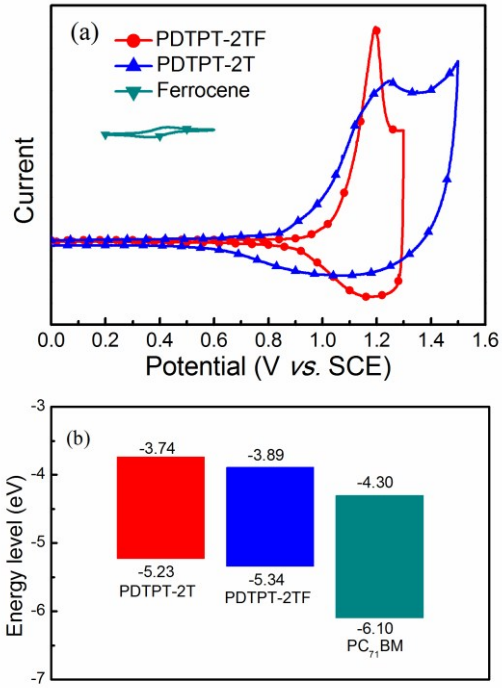

Fig. 3 (a) Electrochemical cyclic voltammograms and (b) energy level diagram of PDTPT-2T and PDTPT-2TF.

respectively. Compared with PDTPT-2T, PDTPT-2TF exhibited pronouncedly down-shifted HOMO and LUMO levels, which should be attributed to the incorporation of electron-withdrawing substituent fluorine. The lower-lying HOMO energy level of PDTPT-2TF is favorable to realizing a higher open-circuit voltage (V_{oc}) in PSCs.[46] The differences of LUMO energy levels between the polymers and [6,6]-phenyl-C_{71}-butyric acid methyl ester ($PC_{71}BM$) are sufficient to guarantee efficient exciton separation at polymer/$PC_{71}BM$ interfaces.[47]

Theoretical calculations

To obtain more information about the molecular conformations and distributions of HOMO and LUMO of PDTPT-2T and PDTPT-2TF, density functional theory (DFT) calculations were performed in the gas phase using Gaussian 09 program at the B3LYP/6-31G (d,p) level. One repeat unit with isobutyl side chains was chosen as the calculating model to reduce the consumption. The optimized molecular geometries were characterized as the minimum-energy conformations by vibrational frequency analysis at the B3LYP/6-31G (d,p) level. Molecule models and backbone dihedral angles of the optimized geometries are shown in Fig. 4. All the optimized geometries of the four molecular models show very small θ_1 and θ_2 values (< 3.5°), indicating that DTPT unit has good planarity. This feature should benefit from C-H ··N and N ··S non-covalent interactions.[4] The values of θ_4 are 15.85° and 18.78° for the non-fluorinated models DTPT-2T-a and DTPT-2T-b, and 1.21° and 0.20° for the fluorinated models DTPT-2TF-a and DTPT-2TF-b, respectively. Incorporating fluorine onto 2T unit significantly reduces the dihedral angle θ_4, which should result from increased

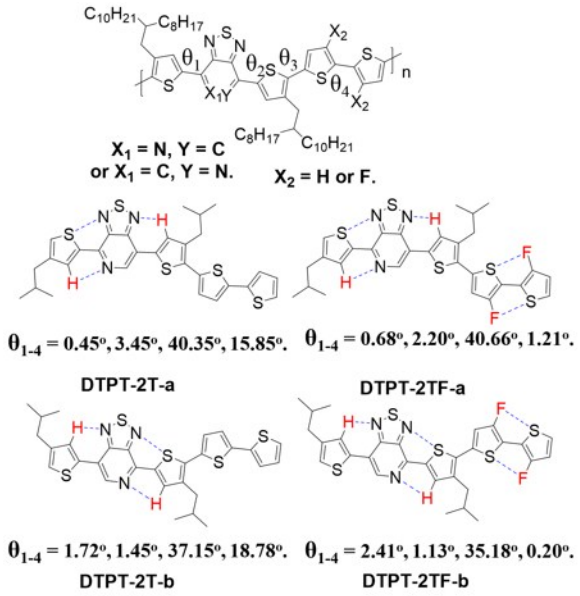

Fig. 4 Molecule models and backbone dihedral angles of optimized geometries obtained by DFT calculations.

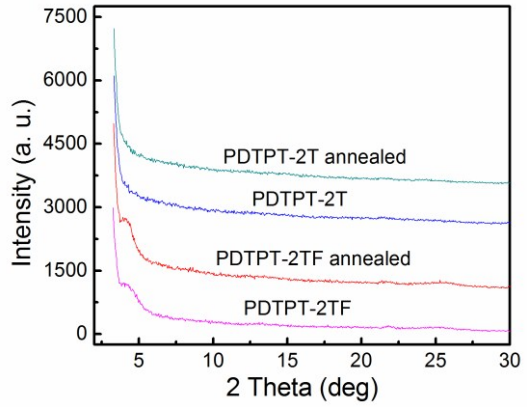

Fig. 5 XRD patterns of PDTPT-2T and PDTPT-2TF films.

intramolecular interaction through F ··S interaction.[4] As shown in Fig. S3, all of the four molecular models exhibit similar HOMO and LUMO distributions: HOMO is distributed along the whole backbone and LUMO is mainly localized on DTPT. Therefore, it is safe to conclude that 2TF remains a donor moiety despite the incorporation of two fluorine atoms.

X-ray diffraction (XRD) analysis

XRD was performed to get a better insight of the effects of fluorine substituent on molecular ordering in solid film. As shown in Fig. 5, neither as-cast nor thermal annealed films of PDTPT-2T showed diffraction peaks, suggesting a more amorphous stacking of PDTPT-2T solid film.[36] In comparison, a diffraction peak centered at ~4.0° could be identified in the XRD patterns of PDTPT-2TF and the peak was strengthened upon annealing, implying the existing of lamellar ordering in PDTPT-2TF film. The corresponding interlamellar distance is ~2.2 nm. Accordingly, PDTPT-2TF exhibits more ordered molecular arrays in film than PDTPT-2T. The amorphous solid

View Article Online
DOI: 10.1039/C6TA04059D

structure of PDTPT-2T may result from the regio-random nature of its backbone. The significantly enhanced non-covalent interactions in PDTPT-2TF through C-H ··F, F ··S, F ··F, and C-F ··π_F interactions, evidenced by UV-vis absorption spectra, are beneficial for forming a more ordered solid structure.[4,48-51]

Solar cell fabrication and performance

Single junction bulk heterojunction (BHJ) PSCs based on the two polymers were fabricated to investigate the effects of fluorine substituent on photovoltaic properties. The configuration of the devices was a typical conventional structure of indium tin oxide (ITO)/poly(3,4-ethylenedioxythiophene): poly(styrenesulfonate) (PEDOT:PSS, ~30 nm)/polymer:$PC_{71}BM$/Ca (~10 nm)/Al (~100 nm). The blend of polymer:$PC_{71}BM$ was stirred in DCB at 100 °C for 2 h before spin coating. In both cases, polymer concentration was 6 mg/mL. The optimized thickness of the active layer was ~67 nm for PDTPT-2T and ~123 nm for PDTPT-2TF.

Fig. 6 depicts the current density-voltage (*J-V*) characteristics of the PSCs with different polymer/acceptor (D/A) ratios. Detailed photovoltaic parameters of the devices are provided in Table 2. The devices based on PDTPT-2T showed very poor photovoltaic performance. The best-performing device only gave a maximum PCE of 2.65%, with a V_{oc} of 0.73 V, a J_{sc} of 5.34 mA/cm^2, and a fill factor (*FF*) of 67.91%. In striking contrast, PDTPT-2TF exhibited excellent photovoltaic performance. The optimum PCEs of the devices based on various D/A ratios were all exceeding 7.50%. A high

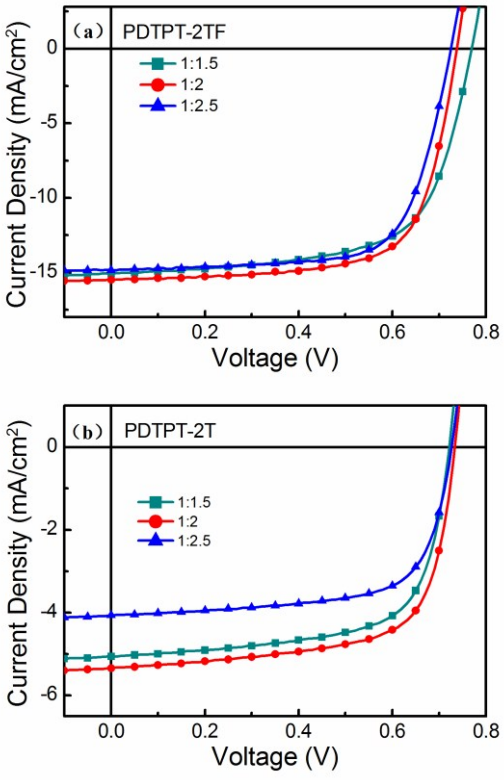

Fig. 6 *J-V* characteristics of the PSCs based on (a) PDTPT-2TF and (b) PDTPT-2T with different polymer/$PC_{71}BM$ ratios.

Table 2 Photovoltaic parameters of the PSCs based on PDTPT-2T and PDTPT-2TF under AM 1.5G illumination (100 mW/cm²)

Polymer	D/A ratio	V_{oc} (V)	J_{sc} (mA/cm^2)	*FF* (%)	PCE_{max} (PCE_{ave})[a] (%)
PDTPT-2T	1:1.5	0.72	5.06	67.14	2.45 (2.14)
	1:2	0.73	5.34	67.91	2.65 (2.51)
	1:2.5	0.73	4.07	68.05	2.02 (1.67)
PDTPT-2TF	1:1.5	0.77	15.07	65.29	7.58 (7.38)
	1:2	0.74	15.52	69.73	8.01 (7.88)
	1:2.5	0.72	14.86	70.01	7.51 (7.44)

[a]The average PCE value was from 5 devices.

V_{oc} of 0.77 V was achieved for 1:1.5 D/A ratio. The improvement of the V_{oc} may benefit from the lower-lying HOMO energy level induced by fluorine substituent. The maximum PCE for PDTPT-2TF was also obtained from 1:2 D/A ratio. Compared with PDTPT-2T-based devices, the devices based on PDTPT-2TF showed a significantly enhanced PCE of 8.01%, along with a slightly higher V_{oc} of 0.74 V, a remarkably enhanced J_{sc} of 15.52 mA/cm^2, and a little higher *FF* of 69.73%. This efficiency is the highest one for PT-containing polymers, and more importantly, it was achieved without any processing additives or post-treatments. The great improvement of photovoltaic performance is mainly ascribed to the significant enhancement of J_{sc}. The thicker active layer, higher absorption coefficient, and broader and bathochromic-shifted absorption, which are all beneficial for harvesting more light, should partially contribute to the significant enhancement of the J_{sc} of PDTPT-2TF-based devices.[1,8,45] For 1:2.5 D/A ratio, the best-performing device based on PDTPT-2TF showed a slightly lower V_{oc} (0.72 V) than that based on PDTPT-2T (0.73 V). Besides the HOMO-LUMO difference between polymer and $PC_{71}BM$, other factors such as shunt resistance, energetic disorder and morphology also play an important role in affecting the V_{oc}.[8,52-55]

For comparison, photovoltaic parameters of the PSCs based on PDTPT-2TF and other reported high-performance PT-containing polymers are summarized in Table 3. PDTPT-2TF-based devices exhibited dramatically enhanced *FF* and PCE in comparison with other PT-containing polymers. To the best of our knowledge, the highest PCE previously reported for PT-containing polymers is only 6.7%, which is obviously lower

Table 3 Photovoltaic parameters of the PSCs based on PDTPT-2TF and other reported high-performance PT-containing polymers

Polymer	V_{oc} (V)	J_{sc} (mA/cm^2)	*FF* (%)	PCE (%)	Reference
PDTPT-2TF	0.74	15.52	69.73	8.01	This work
PDTG-PT	0.59	19.6	57	6.6	36
PIPT-RG	0.88	13.9	55	6.7	43
PBnDT-DTPyT	0.85	12.78	58.2	6.32	32
PNDT-DTPyT	0.71	14.16	61.7	6.20	32
PQDT-DTPyT	0.75	13.49	55.1	5.57	32
PIPCP	0.86	13.4	53	6.13	41
PBPT-12	0.75	12.56	54.2	5.11	42

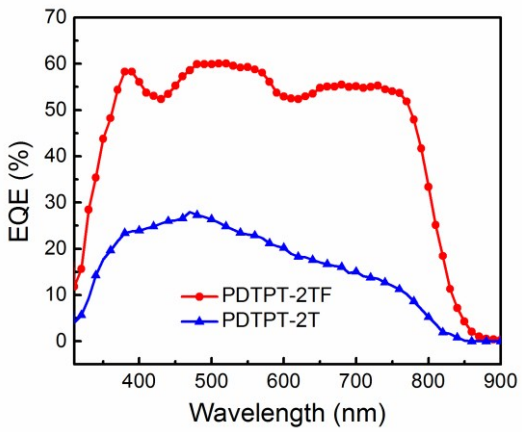

Fig. 7 EQE spectra of the PSCs based on PDTPT-2T and PDTPT-2TF.

than that (8.01%) for PDTPT-2TF.[43] Most of the *FF* values for other PT-containing polymers are below 60% while the *FF* for PDTPT-2TF approached almost 70%, and more importantly, it was achieved without any processing additives or post-treatments. The J_{sc} (15.52 mA/cm^2) for PDTPT-2TF is among the highest ones for PT-containing polymers. From Table 3, it seems that photovoltaic devices based on PT-containing polymers with high J_{sc} values tend to exhibit low V_{oc}. Next work focusing on simultaneously enhancing the V_{oc} and J_{sc} needs to be done to further increase the PCE of PT-containing polymers.

The external quantum efficiencies (EQEs) of the best-performing photovoltaic devices based on PDTPT-2T and PDTPT-2TF were measured and the EQE curves are shown in Fig. 7. The PDTPT-2TF-based device exhibited high EQE values (> 50%) in a very broad wavelength range from 365 to 775 nm, more than two times higher than those of PDTPT-2T-based device. The significant enhancement of EQE indicates noticeably improved charge generation and collection in PDTPT-2TF-based device. The J_{sc} values integrated from the EQE curves are in good agreement with those obtained from the *J-V* measurements.

Hole mobilities of PDTPT-2T:$PC_{71}BM$ (1:2) and PDTPT-2TF:$PC_{71}BM$ (1:2) films were measured by hole-only devices using space-charge-limited current (SCLC) method. The configuration of the devices is ITO/PEDOT:PSS/polymer:$PC_{71}BM$/MoO_3/Al. Fig. S4 shows the dark *J-V* plots of the hole-only devices. The PDTPT-2TF:$PC_{71}BM$ film exhibited about one order of magnitude higher hole mobility (5.63×10^{-4} cm^2/V s) than PDTPT-2T:$PC_{71}BM$ (6.10×10^{-5} cm^2/V s). The higher hole mobility of PDTPT-2TF:$PC_{71}BM$ should also contribute in part to the higher J_{sc} of PDTPT-2TF-based devices.

Morphology study

Active layer morphology plays an important role in affecting the photovoltaic performance. To explore the effects of fluorine substituent on the morphology of active layers, atomic force microscopy (AFM) and transmission electron microscopy (TEM) measurements were performed. AFM and TEM images of the active layers of the best-performing devices are shown in Fig. 8. The PDTPT-2T:$PC_{71}BM$ film showed a rough and

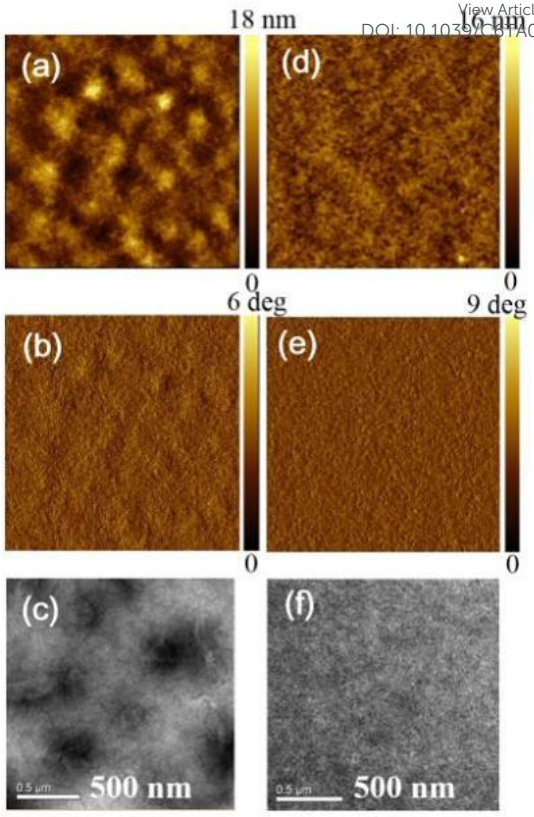

Fig. 8 AFM and TEM images of polymer:$PC_{71}BM$ blends. AFM (a) height image, (b) phase image, and (c) TEM image of PDTPT-2T:$PC_{71}BM$. AFM (d) height image, (e) phase image, and (f) TEM image of PDTPT-2TF:$PC_{71}BM$. The size of the AFM images is 5 μm × 5 μm.

heterogeneous surface with a root-mean-square (RMS) surface roughness of 2.13 nm (Fig. 8a). In contrast, the surface of PDTPT-2TF:$PC_{71}BM$ was smoother and much more homogeneous (RMS = 1.37 nm, Fig. 8d). Previous reports have demonstrated that smooth surface can help reduce leakage current and contact resistance, thus facilitating to yield a high PCE.[56,57] The TEM image (Fig. 8c) of PDTPT-2T:$PC_{71}BM$ suggested that the film was heterogeneous and large polymer-rich and $PC_{71}BM$-rich domains were formed in the film. It is widely believed that: (i) The exciton diffusion length is limited to be ~10 nm, and thus in large domains, inner excitons could hardly reach D/A interfaces before recombination;[29,58,59] (ii) Large phase separation would reduce the contact area of D/A interfaces where excitons separated into free charges.[29] Therefore, the large domains formed in the PDTPT-2T:$PC_{71}BM$ film were detrimental to exciton diffusion and separation, thus resulting in low J_{sc} values. In contrast, PDTPT-2TF showed a good miscibility with $PC_{71}BM$. A homogeneous nanoscale phase separation with appropriate domain sizes can be observed in TEM image (Fig. 8f). Therefore, efficient exciton diffusion and separation could be guaranteed in the PDTPT-2TF:$PC_{71}BM$ blend, facilitating to generate large J_{sc} values. This could also explain why the active layer in PDTPT-2TF-based devices was much thicker than that in PDTPT-2T-based devices. The significant improvement of morphology should be attributed to the incorporation of fluorine into the polymer, which can improve the miscibility between the polymer and

fullerene through reducing the surface energy of the polymer.[50,60,61]

Conclusions

In summary, incorporating fluorine into PT-containing polymer is a very effective strategy to improve the photovoltaic properties. Compared with PDTPT-2T, the fluorinated polymer PDTPT-2TF exhibits obviously enhanced intermolecular interactions, noticeably increased absorption coefficient, broader and bathochromic-shifted absorption, pronouncedly down-shifted LUMO and HOMO energy levels, more ordered solid structure, and significantly improved miscibility with $PC_{71}BM$. These features are conducive to yielding better photovoltaic properties. Conventional photovoltaic devices based on PDTPT-2T only gave a maximum PCE of 2.65%, along with a V_{oc} of 0.73 V, a J_{sc} of 5.34 mA/cm^2, and an *FF* of 67.91% while those based on PDTPT-2TF exhibited a significantly enhanced PCE of 8.01%, with a slightly higher V_{oc} of 0.74 V, a remarkably enhanced J_{sc} of 15.52 mA/cm^2, and a little higher *FF* of 69.73%. The efficiency of 8.01% is the highest one for PT-containing polymers, and more importantly, it is achieved without any processing additives or post-treatments. The easy device processing method for PDTPT-2TF makes it very competitive for potential applications in multicomponent and tandem solar cells. This work indicates that PT would be a promising building block to construct high performance photovoltaic polymers. More in-depth work on stereoregularity of fluorinated PT-containing polymer is undergoing and further enhancement of photovoltaic performance could be expected.

Experimental

Materials

4,7-Dibromo-[1,2,5]thiadiazolo[3,4-*c*]pyridine and monomer 2TF-Sn were purchased from SunaTech Inc. Other chemicals and solvents were obtained from J&K Scientific or Energy Chemical. Tetrahydrofuran (THF) and toluene were dried over sodium/benzophenone. Compound **2**[5,62] and monomer 2T-Sn[63] were prepared according to published procedures. Compound **5** was synthesized using the same procedure as for compound **3**.

Synthetic procedures

Synthesis of 4,7-bis(4-(2-octyldodecyl)thiophen-2-yl)-[1,2,5]thiadiazolo[3,4-*c*]pyridine (3). Anhydrous toluene (40 mL) was added to a mixture of compound **2** (5.88 g, 9 mmol), 4,7-Dibromo-[1,2,5]thiadiazolo[3,4-*c*]pyridine (0.88 g, 3 mmol), and tetrakis(triphenylphosphine)palladium (0.17 g, 0.15 mmol) under an argon atmosphere. The solution was heated to 110 °C and stirred for 48 h. After cooling to room temperature, toluene was removed by rotary evaporation. The crude product was purified by silica gel column chromatography using petroleum ether (PE) and dichloromethane (DCM) as the eluent to afford compound **3** as a red solid (1.82 g, 70% yield). ^{1}H NMR (600 MHz, $CDCl_3$): δ 8.80 (s, 1H), 8.49 (s, 1H), 7.92 (s, 1H), 7.16 (s, 1H), 7.03 (s, 1H), 2.65-2.63 (m, 4H), 1.73-1.70 (m, 2H), 1.36-1.25 (m, 64H), 0.88-0.86 (m, 12H). ^{13}C NMR (150 MHz, $CDCl_3$): δ 154.94, 148.11, 146.38, 143.97, 143.21, 141.16, 140.67, 136.03, 133.63, 129.88, 126.56, 122.85, 120.53, 38.94, 38.91, 35.14, 35.02, 33.38, 31.93, 30.05, 30.04, 29.71, 29.67, 29.37, 27.86, 26.85, 26.66, 22.69, 17.53, 14.11, 13.59.

Synthesis of 4,7-bis(5-bromo-4-(2-octyldodecyl)thiophen-2-yl)-[1,2,5]thiadiazolo[3,4-*c*]pyridine (4). To a mixture of compound **3** (1.23 g, 1.43 mmol), $CHCl_3$ (25 mL), and acetic acid (5 mL), *N*-bromosuccinimide (0.56 g, 3.14 mmol) was added in small portion at room temperature. The reaction was monitored by TLC. After the completion of the reaction, the mixture was poured into 50 mL of distilled water. Then 30 mL of $CHCl_3$ was added and the organic layer was washed with distilled water (3×, 100 mL) and saturated $NaHCO_3$ (1×, 100 mL) sequentially. The solution was dried over anhydrous Na_2SO_4. The solvent was removed by rotary evaporation and the crude product was purified by silica gel column chromatography using PE and DCM as the eluent to give compound **4** as a dark red solid (1.18 g, 81% yield). ^{1}H NMR (600 MHz, $CDCl_3$): δ 8.66 (s, 1H), 8.29 (s, 1H), 7.73 (s, 1H), 2.59-2.56 (m, 4H), 1.77-1.75 (m, 2H), 1.31-1.23 (m, 64H), 0.88-0.85 (m, 12H). ^{13}C NMR (150 MHz, $CDCl_3$): δ 154.57, 147.72, 145.45, 143.46, 142.52, 140.79, 140.13, 135.70, 133.17, 129.11, 119.84, 117.07, 112.55, 38.55, 38.52, 34.41, 34.25, 33.40, 33.38, 31.94, 30.05, 30.04, 29.73, 29.69, 29.66, 29.38, 26.57, 22.71, 14.14.

Synthesis of PDTPT-2TF and PDTPT-2T. Compound **4** (0.2 mmol), 2TF-Sn or 2T-Sn (0.2 mmol), tris(dibenzylideneacetone) dipalladium(0) ($Pd_2(dba)_3$) (3.6 mg, 0.004 mmol), and tri(*o*-tolyl)phosphine (P(*o*-tol)$_3$) (7.2 mg, 0.0236 mmol) were added to a 25 mL round-bottom flask. The mixture was flushed with argon for 30 min. Then anhydrous toluene (5 mL) was added and the solution was flushed with argon for another 30 min. The solution was heated to 110 °C under argon atmosphere. The reaction mixture was cooled to room temperature when the solution became gel. In both cases, the total reaction time was ~2 h. The product was precipitated in methanol and collected by filtration. Crude polymer was extracted by Soxhlet extraction with methanol and chloroform successively. Then the residue was stirred in 100 mL of DCB at 100 °C for 1 h. The solution was filtered through a short path of silica (80−100 mesh). The polymer was obtained by precipitation from methanol and dried under vacuum for 24 h at room temperature.

PDTPT-2T. Yield: 68.72%. M_n: 47 kDa, PDI: 1.67. T_d: 425 °C. Anal. Calcd for C61H89N3S5: C, 71.50; H, 8.75; N, 4.10. Found: C, 71.27; H, 8.68; N, 3.85.

PDTPT-2TF. Yield: 75.28%. M_n: 77 kDa, PDI: 2.01. T_d: 427 °C. Anal. Calcd for C61H87F2N3S5: C, 69.07; H, 8.27; N, 3.96. Found: C, 68.76; H, 8.51; N, 3.62.

Instruments and measurements

The optical absorption spectra of the polymers in solution and as solid films were recorded on a Hitachi U-4100 UV-vis spectrophotometer. Polymer molecular weights were determined by GPC under 40 °C. THF and polystyrene were

View Article Online
DOI: 10.1039/C6TA04059D

used as eluent and standard, respectively. All ^{1}H NMR and ^{13}C NMR spectra were obtained by Bruker DRX-600 spectrometer. Tetramethylsilane (TMS) was used as internal standard. TGA was carried out using a SDT Q600 under a N_2 atmosphere. The polymers were heated from 25 to 800 ^{o}C at a scanning rate of 10 °C/min. Elemental analysis was performed by Vario EL cube. XRD patterns of polymer films were collected on a Hitachi S-4800. The annealed films were prepared by being heated on a hot plate at 100 ^{o}C for 10 min. CV was performed by CHI660D electrochemical workstation with a three-electrode system consisting of Pt electrode (working electrode), Pt wire (counter electrode), and SCE (reference electrode) at a scan rate of 100 mV/s. The electrolyte was tetrabutylammonium hexafluorophosphate (Bu_4NPF_6, 0.1 M) acetonitrile solution. AFM images were obtained by Agilent 5400 in tapping mode. TEM images were obtained by JEOL JEM-1011 at an accelerating voltage of 100 kV. EQE spectra were recorded on a certified Newport incident photon conversion efficiency (IPCE) measurement system.

Fabrication of PSC devices and testing

Single junction BHJ-PSCs were fabricated with a conventional structure of ITO/PEDOT:PSS (~30 nm)/polymer:$PC_{71}BM$/Ca (~10 nm)/Al (~100 nm). ITO-coated glasses were cleaned by sequential ultrasonication in detergent, deionized water, acetone, and isopropyl alcohol. Then they were treated with oxygen plasma for 10 min. PEDOT:PSS (~30 nm) was spin-coated onto the ITO-coated substrates and then dried in an oven at 160 °C for 20 min. The dried substrates were transferred to a N_2 glovebox. Active layer solutions (polymer concentration: 6 mg/mL) were prepared in DCB. The solutions were stirred on a hot plate at 100 °C for 2 h before spin coated onto the hot substrates which were preheated at 100 °C. Under a pressure of 4.0×10^{-4} Pa, Ca (~10 nm) and Al (~100 nm) layers were successively deposited onto the top of active layer. The device active area was 10 mm^2. The *J-V* characteristics of PSCs were measured under AM 1.5G illumination (100 mW/cm^2) using a Keithley 2420 source measurement from a Newport solar simulator. The light intensity was calibrated using a standard silicon photodiode.

Acknowledgements

This work was supported by the Ministry of Science and Technology of China (2014CB643501, 2010DFA52310), and the National Natural Science Foundation of China (21274161, 21402219, 51173199, 51573205 and 61107090).

References

1 C. Liu, K. Wang, X. Gong and A. J. Heeger, *Chem. Soc. Rev.*, 2015, DOI: 10.1039/c5cs00650c.
2 J. Y. Kim, K. Lee, N. E. Coates, D. Moses, T. Q. Nguyen, M. Dante and A. J. Heeger, *Science*, 2007, **317**, 222-225.
3 X. Guo, A. Facchetti and T. J. Marks, *Chem. Rev.*, 2014, **114**, 8943-9021.
4 T. L. Nguyen, H. Choi, S. J. Ko, M. A. Uddin, B. Walker, S. Yum, J. E. Jeong, M. H. Yun, T. J. Shin, S. Hwang, J. Y. Kim, and H. Y. Woo, *Energy Environ. Sci.*, 2014, **7**, 3040-3051.
5 Y. Liu, J. Zhao, Z. Li, C. Mu, W. Ma, H. Hu, K. Jiang, H. Lin, H. Ade and H. Yan, *Nat. Commun.*, 2014, **5**, 5293.
6 J.-H. Kim, M. Lee, H. Yang and D.-H. Hwang, *J. Mater. Chem. A*, 2014, **2**, 6348-6352.
7 H. Yao, W. Zhao, Z. Zheng, Y. Cui, J. Zhang, Z. Wei and J. Hou, *J. Mater. Chem. A*, 2016, DOI: 10.1039/c5ta08614k.
8 J. Wang, M. Xiao, W. Chen, M. Qiu, Z. Du, W. Zhu, S. Wen, N. Wang and R. Yang, *Macromolecules*, 2014, **47**, 7823-7830.
9 J. Zhao, Y. Li, A. Hunt, J. Zhang, H. Yao, Z. Li, J. Zhang, F. Huang, H. Ade and H. Yan, *Adv. Mater.*, 2015, DOI: 10.1002/adma.201504611.
10 M. Zhang, X. Guo, W. Ma, H. Ade and J. Hou, *Adv. Mater.*, 2015, **27**, 4655-4660.
11 L. Han, T. Hu, X. Bao, M. Qiu, W. Shen, M. Sun, W. Chen and R. Yang, *J. Mater. Chem. A*, 2015, **3**, 23587-23596.
12 Z. Li, K. Feng, J. Liu, J. Mei, Y. Li and Q. Peng, *J. Mater. Chem. A*, 2016, **4**, 7372-7381.
13 C. Gu, Q. Zhu, X. Bao, S. Wen, M. Qiu, L. Han, W. Huang, D. Zhu and R. Yang, *Polym. Chem.*, 2015, **6**, 6219-6226.
14 Y. Liu, W. Zhao, Y. Wu, J. Zhang, G. Li, W. Li, W. Ma, J. Hou and Z. Bo, *J. Mater. Chem. A*, 2016, DOI: 10.1039/c6ta02622b.
15 C. E. Small, S. Chen, J. Subbiah, C. M. Amb, S.-W. Tsang, T.-H. Lai, J. R. Reynolds and F. So, *Nat. Photonics*, 2011, **6**, 115-120.
16 S. Liu, K. Zhang, J. Lu, J. Zhang, H. L. Yip, F. Huang and Y. Cao, *J. Am. Chem. Soc.*, 2013, **135**, 15326-15329.
17 T. Yang, M. Wang, C. Duan, X. Hu, L. Huang, J. Peng, F. Huang and X. Gong, *Energy Environ. Sci.*, 2012, **5**, 8208-8214.
18 J. You, L. Dou, K. Yoshimura, T. Kato, K. Ohya, T. Moriarty, K. Emery, C. C. Chen, J. Gao, G. Li and Y. Yang, *Nat. Commun.*, 2013, **4**, 1446.
19 A. R. b. M. Yusoff, D. Kim, H. P. Kim, F. K. Shneider, W. J. da Silva and J. Jang, *Energy Environ. Sci.*, 2015, **8**, 303-316.
20 H. Choi, S. J. Ko, T. Kim, P. O. Morin, B. Walker, B. H. Lee, M. Leclerc, J. Y. Kim and A. J. Heeger, *Adv. Mater.*, 2015, **27**, 3318-3324.
21 T. Ma, K. Jiang, S. Chen, H. Hu, H. Lin, Z. Li, J. Zhao, Y. Liu, Y.-M. Chang, C.-C. Hsiao and H. Yan, *Adv. Energy Mater.*, 2015, DOI: 10.1002/aenm.201501282.
22 K. H. Hendriks, G. H. Heintges, V. S. Gevaerts, M. M. Wienk and R. A. Janssen, *Angew. Chem. Int. Ed.*, 2013, **52**, 8341-8344.
23 L. Dou, C.-C. Chen, K. Yoshimura, K. Ohya, W.-H. Chang, J. Gao, Y. Liu, E. Richard and Y. Yang, *Macromolecules*, 2013, **46**, 3384-3390.
24 J. You, L. Dou, Z. Hong, G. Li and Y. Yang, *Prog. Polym. Sci.*, 2013, **38**, 1909-1928.
25 L. Lu, W. Chen, T. Xu and L. Yu, *Nat. Commun.*, 2015, **6**, 7327.
26 T. Liu, L. Huo, X. Sun, B. Fan, Y. Cai, T. Kim, J. Y. Kim, H. Choi and Y. Sun, *Adv. Energy Mater.*, 2015, DOI: 10.1002/aenm.201502109.
27 W. Li, K. H. Hendriks, A. Furlan, W. S. Roelofs, M. M. Wienk and R. A. Janssen, *J. Am. Chem. Soc.*, 2013, **135**, 18942-18948.
28 H. Zhou, L. Yang, S. Stoneking and W. You, *ACS Appl. Mater. Interfaces*, 2010, **2**, 1377-1383.
29 Y. J. Cheng, S. H. Yang and C. S. Hsu, *Chem. Rev.*, 2009, **109**, 5868-5923.
30 W. Ying, X. Zhang, X. Li, W. Wu, F. Guo, J. Li, H. Ågren and J. Hua, *Tetrahedron*, 2014, **70**, 3901-3908.
31 J. Mao, J. Yang, J. Teuscher, T. Moehl, C. Yi, R. Humphry-Baker, P. Comte, C. Grätzel, J. Hua, S. M. Zakeeruddin, H. Tian and M. Grätzel, *J. Phys. Chem. C*, 2014, **118**, 17090-17099.
32 H. Zhou, L. Yang, S. C. Price, K. J. Knight and W. You, *Angew. Chem. Int. Ed.*, 2010, **49**, 7992-7995.

33 Y. Hua, J. He, C. Zhang, C. Qin, L. Han, J. Zhao, T. Chen, W.-Y. Wong, W.-K. Wong and X. Zhu, *J. Mater. Chem. A*, 2015, **3**, 3103-3112.
34 T. Jiang, Y. Qu, B. Li, Y. Gao and J. Hua, *RSC Adv.*, 2015, **5**, 1500-1506.
35 Y. Hua, H. Wang, X. Zhu, A. Islam, L. Han, C. Qin, W.-Y. Wong and W.-K. Wong, *Dyes Pigments*, 2014, **102**, 196-203.
36 C. P. Yau, Z. Fei, R. S. Ashraf, M. Shahid, S. E. Watkins, P. Pattanasattayavong, T. D. Anthopoulos, V. G. Gregoriou, C. L. Chochos and M. Heeney, *Adv. Funct. Mater.*, 2014, **24**, 678-687.
37 H. Kang, B. Zhao, Z. Cao, J. Zhong, H. Li, Y. Pei, P. Shen and S. Tan, *Eur. Polym. J.*, 2013, **49**, 2738-2747.
38 Y. Sun, S.-C. Chien, H.-L. Yip, Y. Zhang, K.-S. Chen, D. F. Zeigler, F.-C. Chen, B. Lin and A. K. Y. Jen, *J. Mater. Chem.*, 2011, **21**, 13247-13255.
39 N. Blouin, A. Michaud, D. Gendron, S. Wakim, E. Blair, R. Neagu-Plesu, M. Belletête, G. Durocher, Y. Tao and M. Leclerc, *J. Am. Chem. Soc.*, 2008, **130**, 732-742.
40 L. Yang, H. Zhou, S. C. Price and W. You, *J. Am. Chem. Soc.*, 2012, **134**, 5432-5435.
41 M. Wang, H. Wang, T. Yokoyama, X. Liu, Y. Huang, Y. Zhang, T. Q. Nguyen, S. Aramaki and G. C. Bazan, *J. Am. Chem. Soc.*, 2014, **136**, 12576-12579.
42 J. Yuan, X. Huang, H. Dong, J. Lu, T. Yang, Y. Li, A. Gallagher and W. Ma, *Org. Electron.*, 2013, **14**, 635-643.
43 W. Wen, L. Ying, B. B. Hsu, Y. Zhang, T. Q. Nguyen and G. C. Bazan, *Chem. Commun.*, 2013, **49**, 7192-7194.
44 R. C. Coffin, J. Peet, J. Rogers and G. C. Bazan, *Nat. Chem.*, 2009, **1**, 657-661.
45 H. Zhou, L. Yang and W. You, *Macromolecules*, 2012, **45**, 607-632.
46 H.-Y. Chen, J. Hou, S. Zhang, Y. Liang, G. Yang, Y. Yang, L. Yu, Y. Wu and G. Li, *Nat. Photonics*, 2009, **3**, 649-653.
47 M. C. Scharber, D. Mühlbacher, M. Koppe, P. Denk, C. Waldauf, A. J. Heeger and C. J. Brabec, *Adv. Mater.*, 2006, **18**, 789-794.
48 N. E. Jackson, B. M. Savoie, K. L. Kohlstedt, M. Olvera de la Cruz, G. C. Schatz, L. X. Chen and M. A. Ratner, *J. Am. Chem. Soc.*, 2013, **135**, 10475-10483.
49 J. Lee, S. B. Jo, M. Kim, H. G. Kim, J. Shin, H. Kim and K. Cho, *Adv. Mater.*, 2014, **26**, 6706-6714.
50 H. Zhou, L. Yang, A. C. Stuart, S. C. Price, S. Liu and W. You, *Angew. Chem. Int. Ed.*, 2011, **50**, 2995-2998.
51 K. Reichenbacher, H. I. Suss and J. Hulliger, *Chem. Soc. Rev.*, 2005, **34**, 22-30.
52 A. Maurano, R. Hamilton, C. G. Shuttle, A. M. Ballantyne, J. Nelson, B. O'Regan, W. Zhang, I. McCulloch, H. Azimi, M. Morana, C. J. Brabec and J. R. Durrant, *Adv. Mater.*, 2010, **22**, 4987-4992.
53 H. J. Snaith, N. C. Greenham and R. H. Friend, *Adv. Mater.*, 2004, **16**, 1640-1645.
54 G. Garcia-Belmonte and J. Bisquert, *Appl. Phys. Lett.*, 2010, **96**, 113301.
55 J. Liu, Y. Shi and Y. Yang, *Adv. Funct. Mater.*, 2001, **11**, 420-424.
56 R. Lampande, G. W. Kim, J. Boizot, Y. J. Kim, R. Pode and J. H. Kwon, *J. Mater. Chem. A*, 2013, **1**, 6895-6900.
57 S. Han, W. S. Shin, M. Seo, D. Gupta, S.-J. Moon and S. Yoo, *Org. Electron.*, 2009, **10**, 791-797.
58 L. Dong, W. Li and W. S. Li, *Nanoscale*, 2011, **3**, 3447-3461.
59 S. H. Park, A. Roy, S. Beaupré, S. Cho, N. Coates, J. S. Moon, D. Moses, M. Leclerc, K. Lee and A. J. Heeger, *Nat. Photonics*, 2009, **3**, 297-302.
60 J. S. Kim, Y. Lee, J. H. Lee, J. H. Park, J. K. Kim and K. Cho, *Adv. Mater.*, 2010, **22**, 1355-1360.
61 S. Guo, J. Ning, V. Körstgens, Y. Yao, E. M. Herzig, S. V. Roth and P. Müller-Buschbaum, *Adv. Energy Mater.*, 2015, DOI: 10.1002/aenm.201401315.
62 K.-H. Ong, S.-L. Lim, J. Li, H.-K. Wong, H.-S. Tan, T.-T. Lin, L. C. H. Moh, J. C. de Mello and Z.-K. Chen, *Polym. Chem.*, 2013, **4**, 1863-1873.
63 K. Kawabata and H. Goto, *J. Mater. Chem.*, 2012, **22**, 23514-23524.

View Article Online
DOI: 10.1039/C6TA04059D

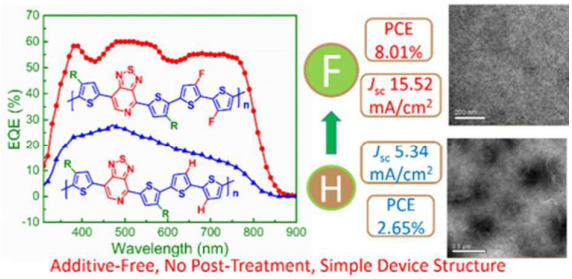

Fluorine substitute was firstly introduced into PT-containing polymer, resulting in significantly improved photovoltaic performance.